PPPL-2079

UC20-F

I, 13590

DR-2136-9

PPPL-2079

PPPL--2079

DE84 007454

FUSION REACTION SPECTRA PRODUCED BY ANISOTROPIC FAST IONS IN THE PLT TOKAMAK

By

W.W. Heidbrink

FEBRUARY 1984

MASTER

PLASMA PHYSICS LABORATORY

PRINCETON UNIVERSITY
PRINCETON, NEW JERSEY

PREPARED FOR THE U.S. DEPARTMENT OF ENERGY,
UNDER CONTRACT DE-AC02-76-CHO-3073.

FUSION REACTION SPECTRA PRODUCED BY ANISOTROPIC FAST IONS IN THE PLT TOKAMAK

W.W. HEIDBRINK
Plasma Physics Laboratory,
Princeton University
Princeton, New Jersey,
United States of America

ABSTRACT

For "beam-target" fusion reactions, collimated measurements of the energy spectrum of one of the reaction products can provide information on the degree of anisotropy of the reacting beam ions. Measurements of the spectrum of 15 MeV protons produced by reactions between energetic ^{3}He ions and relatively cold deuterons during fast wave minority heating in the PLT tokamak indicate that the velocity distribution of fast ^{3}He ions is peaked perpendicular to the tokamak magnetic field.

1. INTRODUCTION

Several authors [1,2] have related the energy distribution of neutrons produced by thermonuclear reactions to the temperature of the reactants, but no analytical treatments and only one [illegible] numerical calculations [3] relating the distribution function of non-thermal reactants [illegible] the energy spectrum of fusion reaction products has been published. In actual controlled fusion experiments, however, the largest fusion reaction rates [4] and the most easily measured fusion spectra are achieved in plasmas with non-thermal populations. [illegible] of these spectra can provide information about the "tail" (non-thermal part) of [illegible] distribution function that may be difficult to obtain using other diagnostic [illegible] date, there have been only a few spectral measurements of fusion neutrons [illegible] with narrowly collimated detectors [5–9], in part due to the massive collimators [illegible] reject scattered neutrons when using conventional detection techniques. [illegible] demonstrated the feasibility of charged fusion product detection in magnetic [illegible] experiments using surface barrier detectors [10,11]. With these detectors, [illegible] tokamak fusion spectra with compact collimation and ~ 100 keV energy [illegible] [10,12].

This paper presents analytical expressions for the fusion energy distribution produced in reactions [illegible] target ions and a monoenergetic, possibly anisotropic, beam for the case of a [illegible] reaction that is isotropic in the center-of-mass (cm) frame. It then applies these expressions to recent measurements of the 15 MeV proton spectrum produced during [illegible] minority heating in the PLT tokamak [13]. The measurements reported here [illegible] the energy resolution of 15 MeV proton spectral measurements made previously on PLT [14], where the highest proton energies were cut off by the finite width of the surface barrier detector. When the full energy of all the protons is measured, the asymmetric, downward-shifted spectrum reported previously becomes a spectrum with two peaks separated by about 2 MeV. Analysis of this spectrum in terms of a model two-component distribution function that has one component purely perpendicular and the other purely isotropic in velocity space indicates that $\gtrsim 90\%$ of the high energy ^{3}He ions created by the waves have velocities perpendicular to the tokamak toroidal field.

2. THEORY

For a reaction 2(1,3)4 where particles 1,2,3,4 are the projectile, target, and products, respectively, the energy of particle 3 using non-relativistic kinematics is [1]

$$E_3 = \frac{m_4}{m_3 + m_4}(Q + K) + V\cos\theta\sqrt{\frac{2m_3m_4}{m_3 + m_4}(Q + K)} + \frac{1}{2}m_3V^2, \tag{1}$$

where Q is the fusion energy, $K = \frac{1}{2}m_1m_2v^2/(m_1+m_2)$ is the relative kinetic energy, $\vec{v} = \vec{v}_1 - \vec{v}_2$ is the relative velocity, $\vec{V} = (m_1\ \vec{v}_1 + m_2\ \vec{v}_2)/(m_1 + m_2)$ is the cm velocity, and θ is the angle between $\vec{V}$ and the cm velocity of particle 3. Our objective is to deduce the energy distribution of product 3, $F(E_3)$, given the reactant distributions $f_1(\vec{v}_1)$ and $f_2(\vec{v}_2)$ and the reaction probability $\sigma v(v,\theta)$. We assume that the fusion cross section is isotropic in angle, i.e., $\sigma = \sigma(v)$, which is valid for the d(t,n) and d(^{3}He,p)α fusion reactions below the resonance energy [15,16]. The d(d,p) and d(d,n) fusion reaction cross sections are of the form [2]

$$\sigma_{dd}(v,\theta) \simeq A(v)\,(1 + B\cos^2\theta), \tag{2}$$

where $B \simeq 0.1$–0.3 so our treatment is only approximately valid for these reactions. In laboratory plasmas, the fusion energy Q is several orders of magnitude larger than the reactant kinetic or cm energy so we order the equation in half-integer powers of the small parameter $\epsilon = m_3V^2/Q$ and neglect terms that enter in order $\epsilon^{\frac{3}{2}}$. For most cases of interest $\sigma(v)$ is a rapidly increasing function of the relative velocity so that the weighting factor $\sigma v f_1(\vec{v}_1)f_2(\vec{v}_2)$ is largest when v is maximized. For ion distributions f_1 and f_2 with comparable velocities, such as in a thermonuclear plasma, v is largest when the reactants collide head on. This implies that most reactions occur with the cm velocity $V \sim 0$, which from Eq. (1) implies that the resulting fusion-product energy distribution is peaked about $E_3 = m_4(Q + K)/(m_3 + m_4)$ [1]. Here, however, we consider the special case of "beam-target" reactions for which $v_1 \gg v_2$, which implies $\sigma(v) \simeq \sigma(v_1)$ independent of $\vec{v}_2$. Under these conditions, it is only the distribution function of the beam and the cross section that determine the fusion-product energy distribution. The general expression for the fusion-product energy distribution function $F(E_3)$ becomes

$$\int_{E_l}^{E_u} F(E_3')\,dE_3' \propto \int \sigma(v_1)v_1 f_1(\vec{v}_1)H(\vec{v}_1)\,d\vec{v}_1, \tag{3}$$

$$\text{where}\quad H(\vec{v}_1) = \begin{cases} 1, & \text{if } E_l < E_3(\vec{v}_1) < E_u; \\ 0, & \text{otherwise.} \end{cases}$$

Due to a particle's fast gyromotion in a magnetically confined plasma, the particle distribution function is independent of direction in the plane perpendicular to the magnetic field, $f(\vec{v}_\perp, v_\parallel) = f(v_\perp, v_\parallel)$. We denote the angle made by the magnetic field vector and the beam particle velocity by χ_1 and the angle between the field and the velocity vector of the fusion product by χ_3. The cm angle θ can be reexpressed in terms of the laboratory angle ϕ between the projectile velocity $\vec{v}_1$ and the product velocity $\vec{v}_3$ according to

$$\cos\theta = \cos\phi - V\sqrt{\frac{m_3(m_3+m_4)}{2m_4Q}}\sin^2\phi + O(\epsilon). \qquad (4$$

Substituting into Eq. (1) yields

$$\begin{aligned} E_3 = {} & \frac{m_4}{m_3+m_4}(Q+K) + V\sqrt{\frac{2m_3m_4}{m_3+m_4}(Q+K)}\cos\phi \\ & + \frac{1}{2}m_3V^2(1-2\sin^2\phi) + O(Q\epsilon^{\frac{3}{2}}). \end{aligned} \qquad (5)$$

The next step is to carry out the angular integration in Eq. (3). Define a reduced fusion-product energy distribution function $\hat{F}(E)$. For the special case of a monoenergetic beam, $f_1(\vec{v}_1) = \delta(v - v_b)g(\vec{v}_1/v_1)$. Since $\hat{F}$ is a monotonic function of the lab frame angle ϕ, $\hat{F}(E) \propto (dE/d\phi)^{-1}g(\phi)$. For an isotropic monoenergetic beam $g(\phi) = \sin\phi$ and

$$\int_{E_l}^{E_u}\hat{F}(E)\,dE = \ln\left(\frac{1+k_0\frac{(E_u-E_0^i)}{\Delta E}}{1+k_0\frac{(E_l-E_0^i)}{\Delta E}}\right)/\ln\left(\frac{1+k_0}{1-k_0}\right), \qquad (6)$$

$$\text{for} \quad |E - E_0^i| < \Delta E,$$

$$\text{where} \quad E_0^i = \frac{m_4}{m_3+m_4}(Q+K) + \frac{1}{2}m_3V^2,$$

$$\Delta E = V\sqrt{\frac{2m_3m_4}{m_3+m_4}(Q+K)}, \quad \text{and}$$

$$k_0 = V\sqrt{\frac{2m_3(m_3+m_4)}{m_4Q}}.$$

For a monoenergetic beam that is unidirectional in pitch angle but isotropic in gyro angle

$$\int_{E_l}^{E_u}\hat{F}(E)\,dE = \frac{1}{\pi}\left[\sin^{-1}\left(\frac{E-E_0^a}{k_1\Delta E}\right) + k_2\sqrt{1-\left(\frac{E-E_0^a}{k_1\Delta E}\right)^2}\right]_{E=E_l}^{E_u} \qquad (7)$$

$$\text{for} \quad |E - E_0^a| < k_1\Delta E,$$

$$\begin{aligned} \text{where} \quad E_0^a &= E_0^i + \Delta E\left[\cos\chi_1\cos\chi_3 - \frac{k_0}{2}(\cos^2\chi_1\sin^2\chi_3 + \sin^2\chi_1\cos^2\chi_3)\right] \\ k_1 &= \sin\chi_1\sin\chi_3(1+k_0\cos\chi_1\cos\chi_3), \quad \text{and} \\ k_2 &= \frac{1}{2}k_0\sin\chi_1\sin\chi_3/(1+k_0\cos\chi_1\cos\chi_3). \end{aligned}$$

The accuracy of Eq. (7) was tested by integrating it numerically over $\sin \chi_1 \, d\chi_1$ to recover the isotropic distribution Eq. (6). The final result for the fusion-product energy distribution function is found by taking the weighted average of reduced distribution functions

$$F(E_3) = \int dE_1 \, \sigma(E_1) E_1 f_1(E_1) \, \hat{F}(E_3, E_1). \tag{8}$$

If the beam distribution function $f_1(E_1)$ decreases rapidly with energy [e.g., if $f_1(E_1)$ is a Boltzmann distribution], then the weighting factor $\sigma(E_1)E_1 f_1(E_1)$ peaks strongly for some energy $E_1 = E_{peak}$ and the fusion-product energy distribution function is approximately

$$F(E_3) \simeq \hat{F}(E_3, E_{peak}). \tag{9}$$

The relation Eq. (9) is useful for qualitative interpretation of 15 MeV proton spectra produced during ICRF heating.

The reduced distribution functions Eqs. (7) and (6) are plotted in Figs. 1a and 1b. The physical origin of the twin lobes (Fig. 1a) for a perpendicular beam distribution viewed in the perpendicular plane is that the probability of a reaction is constant over a gyro period but more of the orbit forms an angle θ near $|\cos\theta| = 1$ than near $\sin\theta = 0$ (Fig. 1c).

3. EXPERIMENT

In the experiment, ^{3}He minority ions were heated in a bulk deuterium plasma by magnetosonic fast waves [13]. 15 MeV protons produced by the d(^{3}He,p)α fusion reaction were detected with a proton spectrometer used previously on PLT [14]. The spectrometer was modified to use a surface barrier detector with a depleted region of 1800 μm, so that protons with energies up to 20 MeV deposited their full energy in the depleted region of the detector. The previous apparatus only collected the full energy of protons with less than 15.5 MeV. The spectrometer was collimated to measure perpendicular protons (collimator FWHM = 6.5°) produced in the plasma between major radii of approximately 102 cm and 140 cm, with nearly constant detection efficiency over this range [14]. The ^{3}He cyclotron layer was at major radii of 125–143 cm for these discharges.

The measured 15 MeV proton spectra exhibit a broad, two-lobed structure (Fig. 2a) for discharges characterized by plasma currents of 500–550 kA, toroidal fields of 28–32 kG, line-average electron densities of 1.7–3.0 x 10^{13} cm^{-3}, ICRF powers of 100–500 kW at 30 MHz, and d(^{3}He,p)α reaction rates of $\gtrsim 10^{11}$ sec^{-1}. In contrast, co-injection of a 40 keV deuterium neutral beam into a deuterium and ^{3}He plasma in the absence of ICRF produced a relatively narrow 15 MeV proton spectrum with a single peak (Fig. 2b). The width of the proton spectrum during ICRF was found to depend less sensitively on electron density, ICRF power, toroidal magnetic field, and ^{3}He density than the d(^{3}He,p)α reaction rate (Fig. 3). Operation of the spectrometer was restricted to a relatively narrow parameter regime by the requirement that the reaction rate be sufficiently large for statistically significant measurements but sufficiently small to avoid appreciable pulse pile-up The ratio of counts in the low energy peak to the number of counts in the central minimu was 1.68 ± 0.29 for discharges with full spectral width ≥ 2.7 MeV; the ratio of counts in the high energy peak to counts in the central minimum was 1.38 ± 0.22.

4. DISCUSSION

A twin-lobed spectrum cannot be produced by an isotropic beam. Although these spectral measurements of protons at a single angle of escape do not provide enough information to determine uniquely the direction of anisotropy of the ^{3}He tail, they are consistent with theoretical predictions of a perpendicular anisotropic tail [14,17]. The spacing of the lobes implies that perpendicular ^{3}He ions with energy of ~ 40 keV in the case of the most closely spaced peaks and ~ 300 keV in the case of the most widely spaced peaks made the dominant contribution to the observed proton spectra. Theoretically, the ^{3}He distribution is predicted to be perpendicular for energies $\gtrsim 20 Z_{eff}^{\frac{2}{3}} T_e \sim 30$ keV [17]. The instrumental resolution was too poor in these experiments to determine the minimum energy at which anisotropy exists. The ratio of counts between lobes to the number of counts in the peaks implies that the isotropic contribution to the observed spectrum is less than 10% of the perpendicular contribution.

The observation that the proton spectral width is less sensitve to the parameters affecting ^{3}He tail heating than the d(^{3}He,p)α reaction rate (Fig. 3) is consistent with theoretical expectations. Asymptotic analysis [18] of Eq. (8) using an analytical fit to the cross section σ [19] and the assumed ^{3}He distribution function $f_1(E_1) \propto \exp(-E/T)$, where T is the tail temperature, indicates that the energy E_{peak} for which the weighting factor $\sigma E f$ is maximized depends on tail temperature according to $E_{peak} \simeq 14(\text{keV})^{\frac{1}{3}} T^{\frac{2}{3}}$. This implies that the spectral width scales approximately as $T^{\frac{1}{3}}$. In contrast to this weak algebraic dependence on tail temperature, the analysis predicts a strong exponential dependence of the d(^{3}He,p)α reaction rate R_{dHe} on tail temperature, $R_{dHe} \sim \exp[-43(\text{keV}/T)^{\frac{1}{3}}]$. The reaction rate also depends on the number density of ^{3}He tail ions, while the proton spectrum produced by the minority tail depends on tail temperature alone. Combining expressions, the spectral width W is expected to scale with reaction rate R and ^{3}He density n as

$$W_2 = W_1[1 + 0.023T_i^{\frac{1}{3}} \ln(\frac{n_2 R_1}{n_1 R_2})]^{-1}. \tag{10}$$

The predictions of Eq. (10) are plotted in Fig. 3 using the measured value of the reaction rate and a single normalization ($W_1 = 3.0$MeV, $R_1 = 4 \times 10^{11}$sec^{-1}, $n_1 \simeq 1.0 \times 10^{12}$cm^{-3}. $T_i \simeq 40$keV is implied by $W_1 = 3.0$ MeV). A major uncertainty in the application of Eq. (10) is determination of the ^{3}He density, which was estimated from the rise in electron density when neutral ^{3}He was puffed into the vacuum vessel $\sim$ 50 ms prior to the ICRF pulse, but which differs from this value due to ^{3}He pumping and desorption [20]. The measured scaling of spectral width with reaction rate is consistent with the theoretical prediction of Eq. (10) within the experimental error (Fig. 3). When the ^{3}He gas puff was reduced so that the density rise was below the minimum detectable level ($\Delta\ \bar{n}_e \lesssim 0.2 \times 10^{12}$cm^{-3}) (Fig. 3d), the spectral width broadened slightly, implying that the tail temperature continued to rise with decreasing ^{3}He concentration; but the reaction rate fell, implying that the reduction in number density of ^{3}He ions had a stronger effect on the reaction rate than the increase in tail temperature.

The probable explanation for the asymmetric, downward-shifted proton spectra observed previously in PLT [14] is that the thinner detector used in those experiments failed to collect the full energy of the protons in the upper lobe of the distribution (Fig. 4).

5. CONCLUSION

Measurements of the spectrum of 15 MeV protons produced during fast wave minority heating in the PLT tokamak indicate that $\gtrsim 90\%$ of $\sim$ 200 keV ^{3}He ions near the major radius of the device are anisotropic in velocity space. The width of the proton spectrum is increased by increasing the RF power, by reducing the electron or ^{3}He density, and by adjusting the toroidal field so that the ^{3}He resonance layer is in the center of the discharge, but measurements of the d(^{3}He,p)α reaction rate are much more sensitive to changes in tail temperature than are the spectral measurements. The tail temperature implied by the spectral measurements is typically between 30 and 50 keV.

ACKNOWLEDGMENTS

The author thanks J.D. Strachan for suggesting this problem and for critically reading the manuscript and G. Hammett, R.E. Chrien, D. Hwang, and D. Slaughter for helpful discussions. H.H.Towner graciously shared his notes and G. Estepp provided technical assistance. The support of the PLT and ICRF groups under J. Hosea and the Neutral Beam group under G. Schilling are gratefully acknowledged, with special credit due J.R. Wilson and P. Colestock for forming the plasmas diagnosed in this experiment. This work was supported by U.S. Department of Energy Contract No. DE-AC02-76-CHO-3073.

References

[1] BRYSK, H., Plasma Physics 15 (1973) 611, and references therein.

[2] LEHNER, G., POHL, F., Neutrons from D-D Reactions as a Tool for Plasma Diagnostics, Inst. Plasmaphysik Rep. IPP I/60 (1967).

[3] TOWNER, H.H., JASSBY, D.L., Trans. Am. Nucl. Soc. 22 (1975) 74.

[4] STRACHAN, J.D., et al., in K.H. Bockhoff (ed.), *Nuclear Data for Science and Technology* (ECSC, Brussels, 1983) 313.

[5] CONNER, J.P., et al., in Proc. 2nd U.N. Conf. (United Nations, Geneva, 1958) 32, 297.

[6] ROSE, B., et al., Nature 181 (1958) 1630.

[7] STRACHAN, J.D., et al., Nature 279 (1979) 626.

[8] WAGNER, F., et al., in *Plasma Physics and Controlled Nuclear Fusion Research* (IAEA, Baltimore, 1983) Vol. I, 43.

[9] GOLUBEV, V.I., et al., JETP Lett. 37 (1983) 20.

[10] FOOTE, J.H., Nucl. Fusion 19 (1979) 1215.

[11] CHRIEN, R.E., et al., Phys. Rev. Lett **46** (1981) 535.

[12] HWANG, D.Q., et al., in *Plasma Physics and Controlled Nuclear Fusion Research* (IAEA, Baltimore, 1983) Vol. II, 3.

[13] HOSEA, J., et al., in *Plasma Physics and Controlled Nuclear Fusion Research* (IAEA, Vienna, 1981), Vol. II, 95.

[14] CHRIEN, R.E., STRACHAN, J.D., Phys. Fluids 26 (1983) 1953.

[15] CONNER, J.P., BONNER, T.W., SMITH, J.R., Phys. Rev. **88** (1952) 468.

[16] BONNER, T.W., CONNER, J.P., LILLIE, A.B., Phys. Rev. **88** (1952) 473.

[17] STIX, T.H., Nucl. Fusion 15 (1975) 737.

[18] A similar analysis for the d(d,n) fusion reaction is found in POST, R.F., Revs. Modern Phys. 28 (1956) 338.

[19] MILEY, G.H., TOWNER, H., IVICH, N., Fusion Cross Section and Reactivities, Rept. COO-2218-17 (University of Illinois, Urbana, Ill., 1974).

[20] CHRIEN, R.E., et al., Nucl. Fusion **21** (1981) 1661.

[21] CHRIEN, R.E., Ph.D. Thesis, Princeton University, 1982, 46.

Figure Captions

Fig. 1a. Spectrum of protons emitted perpendicular to the magnetic field ($\chi_3 = \pi/2$) by $d(^3He,p)\alpha$ fusion reactions between an anisotropic ($\chi_1 = \pi/2$), monoenergetic (200 keV) ^3He beam and a cold deuterium plasma. The asymmetry between the higher energy and lower energy peaks originates in the transformation from the cm frame to the laboratory frame.

Fig. 1b. Spectrum of protons emitted perpendicular to the magnetic field by $d(^3He,p)\alpha$ fusion reactions between an isotropic monoenergetic (200 keV) ^3He beam and a cold deuterium plasma.

Fig. 1c. Physical explanation for the twin-lobed structure of a proton spectrum produced by an anisotropic perpendicular beam. Although the probability that a reaction occurs is constant during a beam ion's circular gyromotion, $\vec{v}_1 \cdot \vec{v}_3$ does not vary uniformly during a gyro period, causing more ions to be emitted with a maximal Doppler shift than without any shift.

Fig. 2a. Proton spectrum during ^3He minority ICRF heating (240 kW) in a discharge with $I_\phi \simeq 500\,kA$, $\bar{n}_e = 2.7 \times 10^{13} cm^{-3}$, and $B_\phi = 30.5\,kG$. The curve is the spectrum produced by an anisotropic perpendicular ^3He beam with maximum energy of 400 keV and temperature of 30 keV. The absolute accuracy of the energy measurement is $\pm 2.5\%$; the resolution of the spectrometer is 0.5 MeV (full line-width).

Fig. 2b. Proton spectrum during co-injection of a 40 keV deuterium neutral beam into a deuterium and ^3He plasma in the absence of ICRF. The curve is the spectrum produced by an isotropic 40 keV deuterium beam with a classical slowing-down distribution ($f(v) \propto v^{-3}$).

Fig. 3. 15 MeV proton spectral width and $d(^3He,p)\alpha$ reaction rate versus line-average electron density (a), toroidal field (b), ICRF power (c), and estimated line-average ^3He density (d) with the other parameters held constant. $I_\phi \simeq 500kA$. The dashed curve through the reaction rate data is the fit used to calculate the spectral width predicted by the asymptotic analysis of Sec. 4 (solid curves).

Fig. 4. A good fit to the asymmetric proton spectrum measured previously [14] is found by assuming that the true proton spectrum was produced by an anisotropic perpendicular ^3He beam with maximum energy 400 keV and temperature 50 keV but that

this spectrum was distorted by a thin detector with the model response

$$E_{det} = \begin{cases} E_p, & \text{if } E_p \leq 15.4 MeV; \\ 3(15.4MeV - 2E_p), & \text{if } E_p > 15.4MeV. \end{cases}$$

The model detector response is based on calculations summarized in Fig. 2.5 of [21]. The counts below 12.5 MeV in the data are thought to be protons that lose energy in the walls of the collimator.

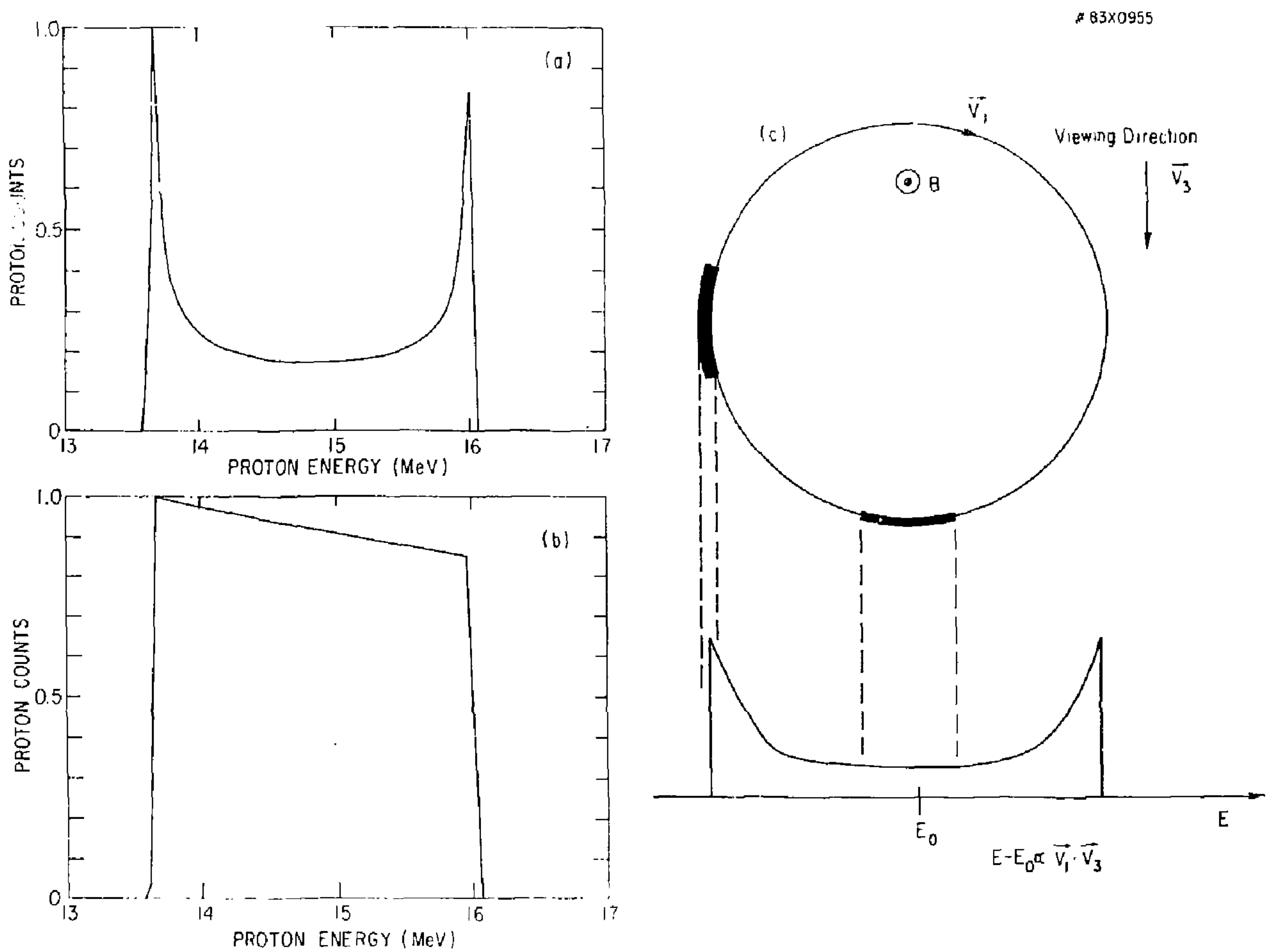

83X0955
(a)
PROTON COUNTS
PROTON ENERGY (MeV)
(b)
PROTON COUNTS
PROTON ENERGY (MeV)
(c)
$\vec{V_1}$
Viewing Direction
$\vec{V_3}$
B
E_0
E
$E-E_0 \propto \vec{V_1}\cdot\vec{V_3}$

Fig. 1

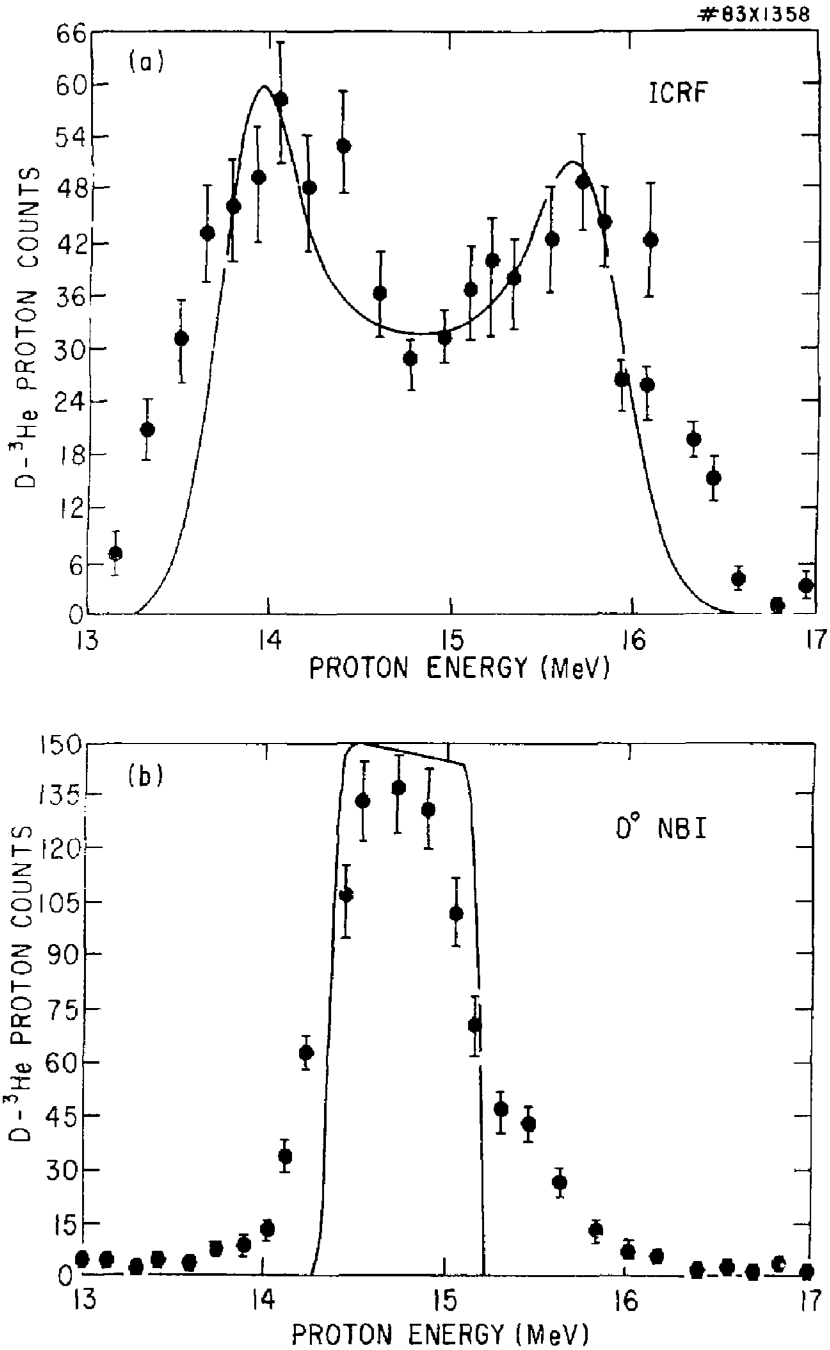
#83X1358
(a)
ICRF
D-3He PROTON COUNTS
66
60
54
48
42
36
30
24
18
12
6
0
13
14
15
16
17
PROTON ENERGY (MeV)
(b)
D° NBI
D-3He PROTON COUNTS
150
135
120
105
90
75
60
45
30
15
0
13
14
15
16
17
PROTON ENERGY (MeV)

Fig. 2

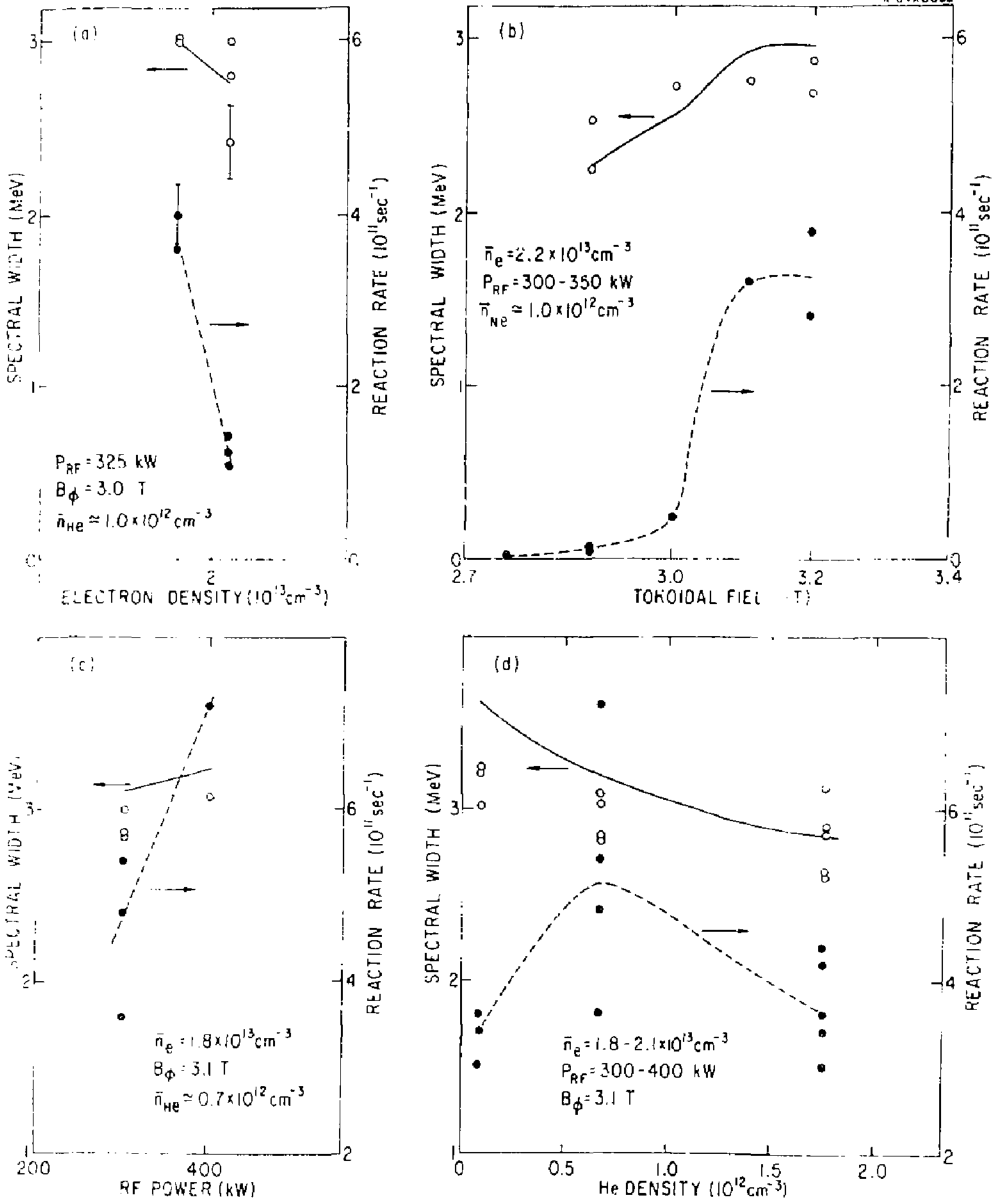

(a)
SPECTRAL WIDTH (MeV)
REACTION RATE (10^{11} sec^{-1})
P_{RF} = 325 kW
B_ϕ = 3.0 T
$\bar{n}_{He} \simeq 1.0\times10^{12}$ cm^{-3}
ELECTRON DENSITY (10^{13}cm^{-3})
(b)
$\bar{n}_e$ = 2.2 × 10^{13}cm^{-3}
P_{RF} = 300 - 350 kW
$\bar{n}_{He} \simeq 1.0\times10^{12}$ cm^{-3}
2.7
3.0
3.2
3.4
(c)
$\bar{n}_e$ = 1.8×10^{13}cm^{-3}
B_ϕ = 3.1 T
$\bar{n}_{He} \simeq 0.7\times10^{12}$ cm^{-3}
200
400
RF POWER (kW)
(d)
$\bar{n}_e$ = 1.8 - 2.1×10^{13}cm^{-3}
P_{RF} = 300 - 400 kW
B_ϕ = 3.1 T
0
0.5
1.0
1.5
2.0
He DENSITY (10^{12}cm^{-3})

Fig. 3

#83X0954

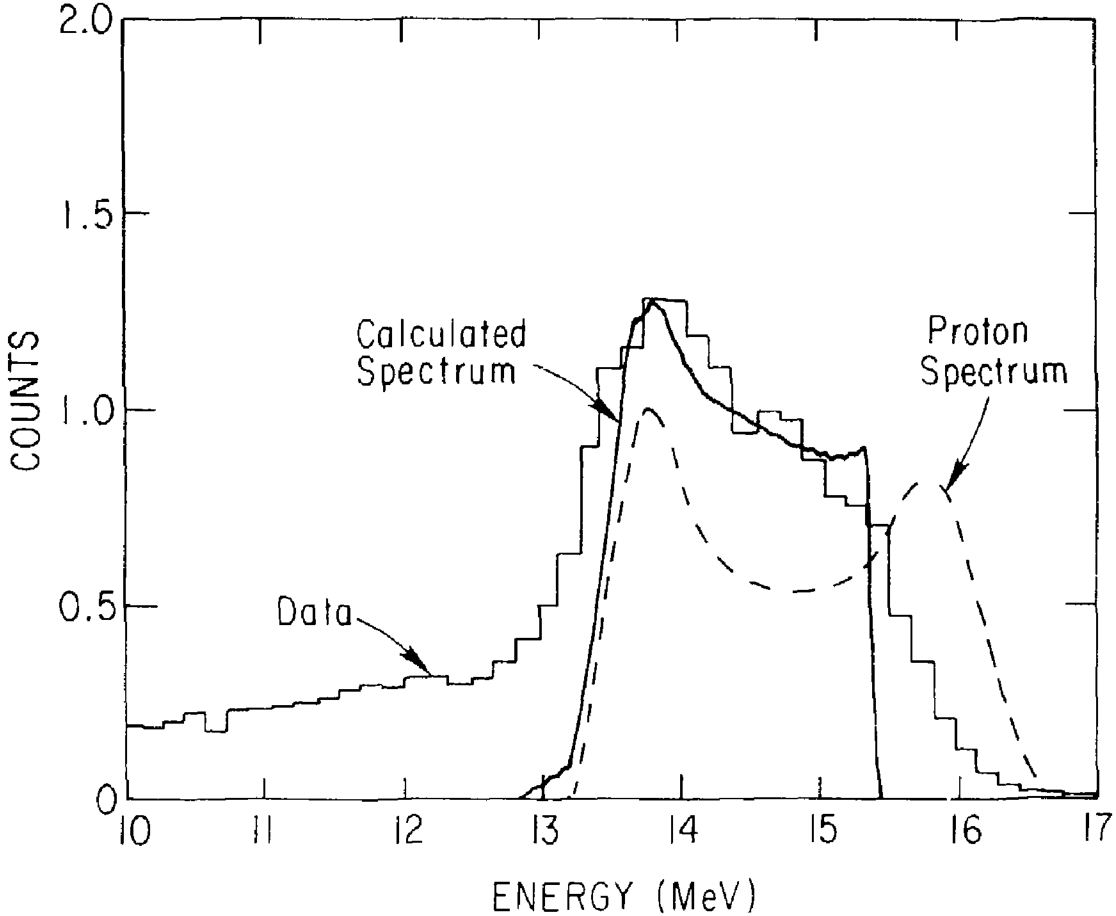

2.0
1.5
1.0
0.5
0
COUNTS
10
11
12
13
14
15
16
17
ENERGY (MeV)
Calculated
Spectrum
Proton
Spectrum
Data

EXTERNAL DISTRIBUTION IN ADDITION TO TIC UC-20

Plasma Res Lab, Austra Nat'l Univ, AUSTRALIA
Dr. Frank J. Paoloni, Univ of Wollongong, AUSTRALIA
Prof. I.R. Jones, Flinders Univ., AUSTRALIA
Prof. M.H. Brennan, Univ Sydney, AUSTRALIA
Prof. F. Cap, Inst Theo Phys, AUSTRIA
Prof. Frank Verheest, Inst theoretische, BELGIUM
Dr. D. Palumbo, Dg XII Fusion Prog, BELGIUM
Ecole Royale Militaire, Lab de Phys Plasmas, BELGIUM
Dr. P.H. Sakanaka, Univ Estadual, BRAZIL
Dr. C.R. James, Univ of Alberta, CANADA
Prof. J. Teichmann, Univ of Montreal, CANADA
Dr. H.M. Skarsgard, Univ of Saskatchewan, CANADA
Prof. S.R. Sreenivasan, University of Calgary, CANADA
Prof. Tudor W. Johnston, INRS-Energie, CANADA
Dr. Hannes Barnard, Univ British Columbia, CANADA
Dr. M.P. Bachynski, MPB Technologies, Inc., CANADA
Zhengwu Li, SW Inst Physics, CHINA
Library, Tsing Hua University, CHINA
Librarian, Institute of Physics, CHINA
Inst Plasma Phys, Academia Sinica, CHINA
Dr. Peter Lukac, Komenskeho Univ, CZECHOSLOVAKIA
The Librarian, Culham Laboratory, ENGLAND
Prof. Schatzman, Observatoire de Nice, FRANCE
J. Radet, CEN-BP6, FRANCE
AM Dupas Library, AM Dupas Library, FRANCE
Dr. Tom Mual, Academy Bibliographic, HONG KONG
Preprint Library, Cent Res Inst Phys, HUNGARY
Dr. S.K. Trehan, Panjab University, INDIA
Dr. Indra, Mohan Lal Das, Banaras Hindu Univ, INDIA
Dr. L.K. Chavda, South Gujarat Univ, INDIA
Dr. R.K. Chhajlani, Var Ruchi Marg, INDIA
P. Kaw, Physical Research Lab, INDIA
Dr. Phillip Rosenau, Israel Inst Tech, ISRAEL
Prof. S. Cuperman, Tel Aviv University, ISRAEL
Prof. G. Rostagni, Univ Di Padova, ITALY
Librarian, Int'l Ctr Theo Phys, ITALY
Miss Clelia De Palo, Assoc EURATOM-CNEN, ITALY
Biblioteca, del CNR EURATOM, ITALY
Dr. H. Yamato, Toshiba Res & Dev, JAPAN
Prof. M. Yoshikawa, JAERI, Tokai Res Est, JAPAN
Prof. T. Uchida, University of Tokyo, JAPAN
Research Info Center, Nagoya University, JAPAN
Prof. Kyoji Nishikawa, Univ of Hiroshima, JAPAN
Prof. Sigeru Mori, JAERI, JAPAN
Library, Kyoto University, JAPAN
Prof. Ichiro Kawakami, Nihon Univ, JAPAN
Prof. Satoshi Itoh, Kyushu University, JAPAN
Tech Info Division, Korea Atomic Energy, KOREA
Dr. R. England, Civdad Universitaria, MEXICO
Bibliotheek, Fom-Inst Voor Plasma, NETHERLANDS
Prof. B.S. Liley, University of Waikato, NEW ZEALAND
Dr. Suresh C. S[illegible]rma, Univ of Calabar, NIGERIA
Prof. J.A.C. Cabral, Inst Superior Tech, PORTUGAL
Dr. Octavian Petrus, ALI CUZA University, ROMANIA
Prof. M.A. Hellberg, University of Natal, SO AFRICA
Dr. Johan de Villiers, Atomic Energy Bd, SO AFRICA
Fusion Div, Library, JEN, SPAIN
Prof. Hans Wilhelmson, Chalmers Univ Tech, SWEDEN
Dr. Lennart Stenflo, University of UMEA, SWEDEN
Library, Royal Inst Tech, SWEDEN
Dr. Erik T. Karlson, Uppsala Universitet, SWEDEN
Centre de Recherchesen, Ecole Polytech Fed, SWITZERLAND
Dr. W.L. Weise, Nat'l Bur Stand, USA
Dr. W.M. Stacey, Georg Inst Tech, USA
Dr. S.T. Wu, Univ Alabama, USA
Prof. Norman L. Oleson, Univ S Florida, USA
Dr. Benjamin Ma, Iowa State Univ, USA
Prof. Magne Kristiansen, Texas Tech Univ, USA
Dr. Raymond Askew, Auburn Univ, USA
Dr. V.T. Tolok, Kharkov Phys Tech Ins, USSR
Dr. D.D. Ryutov, Siberian Acad Sci, USSR
Dr. G.A. Eliseev, Kurchatov Institute, USSR
Dr. V.A. Glukhikh, Inst Electro-Physical, USSR
Institute Gen. Physics, USSR
Prof. T.J. Boyd, Univ College N Wales, WALES
Dr. K. Schindler, Ruhr Universitat, W. GERMANY
Nuclear Res Estab, Julich Ltd, W. GERMANY
Librarian, Max-Planck Institut, W. GERMANY
Dr. H.J. Kaeppler, University Stuttgart, W. GERMANY
Bibliothek, Inst Plasmaforschung, W. GERMANY